Matrix Reactivity of Al and Ga Atoms (M) in the Presence of Silane: Generation and Characterization of the η^2-Coordinated Complex M·SiH_4, the Insertion Product $HMSiH_3$, and the M^I Species $MSiH_3$ in a Solid Argon Matrix

Benjamin Gaertner,[a] Hans-Jörg Himmel,*[a] Victoria A. Macrae,[b] Anthony J. Downs,[b] and Tim M. Greene[c]

Abstract: Matrix isolation experiments give evidence for the formation of the loosely bonded metal–silane complex M·SiH_4 by the spontaneous reaction of Al or Ga atoms (M) with silane in a solid Ar matrix at 12 K; however, Ga_2 appears to insert spontaneously into an Si–H bond to form $HGaGaSiH_3$, probably with the structure HGa(μ-SiH_3)Ga. In M·SiH_4 the metal atom is η^2-coordinated by the silane, resulting in a species with C_{2v} symmetry. The complex has a distinctive photochemistry: it can be converted on photolysis at $\lambda \approx 410$ or ≈ 254 nm to its tautomer, $HMSiH_3$, which also has a doublet ground electronic state and from which it can be regenerated with $\lambda \approx 580$ nm radiation. Broadband UV-visible photolysis ($\lambda = 200$–800 nm) results in decomposition of $HMSiH_3$, the univalent species $MSiH_3$ being the only detectable product. The experimental data collected for several silane isotopomers (SiH_4, SiD_4, and SiD_3H) and different reagent concentrations, together with the results of sophisticated quantum chemical calculations, are used to explore in detail the properties of the detected species and the reaction pathways compassing their formation.

Keywords: aluminum · gallium · matrix isolation · silanes · structure elucidation

Introduction

Several complexes in which the CH_4 or SiH_4 molecule is coordinated to a transition-metal center have now been authenticated. Such complexes excite attention mainly for their relevance to C–H and Si–H bond activation, and their properties are likely to be crucial to a proper understanding of these processes.[1] Examples include species in which the CH_4 or SiH_4 is coordinated to one metal center as, for example, in the first η^2-SiH_4 transition-metal complex to be characterized, *cis*-[Mo(η^2-SiH_4)(CO)($R_2PC_2H_4PR_2$)$_2$] (R = Ph, *i*Bu, Et),[2] and others in which the CH_4 or SiH_4 is trapped between two metal centers, as in [$(R_3P)_2H_2Ru(SiH_4)$-$RuH_2(PR_3)_2$] (R = Cy or *i*Pr).[3] Remarkably, *cis*-[Mo(η^2-SiH_4)(CO)($Et_2PC_2H_4PEt_2$)$_2$] is reported[2] to enter into equilibrium with its tautomer [MoH(SiH_3)(CO)($Et_2PC_2H_4$-PEt_2)$_2$], which features a seven-coordinate Mo center, as evidenced by the ^{1}H and ^{31}P NMR spectra of the solutions at different temperatures. Quantum chemical studies indicate that bonding in these SiH_4 complexes occurs through 1) a dative bond involving the σ(Si–H) orbital and a vacant metal (M) orbital of appropriate symmetry, and 2) d(M)$\rightarrow$ σ^*(Si–H) back-donation.

By contrast, little is known about complexes of SiH_4 or CH_4 with main-group elements, for which the interaction is expected to be much weaker. The reaction of O atoms, produced by O_3 photolysis, with SiH_4 leads immediately to insertion with the formation of $HOSiH_3$ together with other products.[4] Photoexcitation is a precondition for the formation of $HSiCH_3$ from Si atoms and CH_4, whereas Si atoms react spontaneously with SiH_4 to give $HSiSiH_3$ and Si_2H_4.[5] Hg atoms have also been shown to react with SiH_4 upon photoactivation: insertion gives $HHgSiH_3$, as well as other secondary products, but no trace has been found of a complex of the form Hg·SiH_4,[6] although calculations predict a bonding energy of no less than 29.7 kJ mol^{-1}.[7] Detailed analysis of the IR spectra of gaseous van der Waals complexes featuring Ar[8] or Ne[9] coordinated to SiH_4 gives

[a] B. Gaertner, Dr. H.-J. Himmel
Institut für Anorganische Chemie der Universität Karlsruhe
Engesserstrasse, Geb. 30.45, 76128 Karlsruhe (Germany)
Fax: (+49) 721-608-4854

[b] V. A. Macrae, Prof. A. J. Downs
Inorganic Chemistry Laboratory, University of Oxford
South Parks Road, Oxford OX1 3QR (UK)

[c] Dr. T. M. Greene
Department of Chemistry, University of Exeter
Stocker Road, Exeter EX4 4QD (UK)

Supporting information for this article is available on the WWW under http://www.chemeurj.org/ or from the author.

  DOI: 10.1002/chem.200305493

some grounds for believing that an energy minimum is achieved by positioning the noble gas atom near one of the midpoints of the six edges of the SiH_4 tetrahedron. Rather more strongly bonded complexes of silanes with molecules such as NH_3, HF, or HONO have also been characterized, for example, SiH_4,[10] SiF_4,[11] or $HSiCl_3$[12] with NH_3; SiH_4, Si_2H_6, CH_3SiH_3, $(CH_3)_2SiH_2$, or $(CH_3)_3SiH$ with HF;[13] and SiH_4 with HONO.[14]

Previous experiments with Group 13 metal atoms (M) in an Ar matrix doped with CH_4 revealed[15,16] that UV photolysis causes insertion of M into a C–H bond, with the formation of the photolabile M^{II} product $HMCH_3$, where M = Al, Ga, or In. However, they give no spectroscopic sign of the CH_4 complex that might be expected to be the precursor to this reaction. The more polarizable SiH_4 molecule is undoubtedly a better prospect for forming a metal atom complex that is sufficiently strongly bonded to be detected spectroscopically in the presence of an excess of free SiH_4. Earlier experiments with Al atoms in an Ar matrix at ≈12 K certainly left no doubt about their potential, upon photoexcitation, to activate SiH_4 and so give rise to the Al^{II} species $HAlSiH_3$.[17] In a very recent preliminary communication,[18] some of us have presented IR evidence that co-deposition of Al and SiH_4 under these conditions yields initially a weakly bonded metal atom complex Al·SiH_4, whose physical and photochemical properties have been outlined. Here we give a more detailed account of these experiments, which have now been augmented with the investigation of the behavior of not only Al but also Ga atoms. Quantum chemical calculations identify three different isomers of the 1:1 complex M·SiH_4 formed by the metal atom M (M = Al or Ga) in its ^2P ground electronic state, with little difference in energy between them. In practice, according to a detailed analysis of the IR spectra displayed by the complexes associated with the different isotopomers SiH_4, SiD_4, and SiD_3H, the preferred configuration involves coordination through one edge of the SiH_4 tetrahedron, that is, M(η^2-H_2SiH_2). The "isolated" ν(Si–H) modes[19] of the SiD_3H complexes provide a direct experimental measure of the degree of perturbation experienced by the silane molecule; this is reproduced well by calculations at an appropriate level of theory. The experiments show, moreover, that tautomerization of the complex to the M^{II} derivative $HMSiH_3$, brought about by irradiation at wavelengths near 410 nm and also at λ = 254 nm, can be reversed by moving the photolyzing radiation to wavelengths near 580 nm. With broadband UV-visible photolysis, however, the univalent derivative $MSiH_3$ of the metal is believed to be the ultimate product. By contrast with atomic Ga, however, the Ga_2 dimer reacts spontaneously with SiH_4 with insertion into an Si–H bond to form a product, most probably with the formulation HGa(μ-SiH_3)Ga.

Experimental Section

Evaporation of aluminum (Merck; purity 99.99%) or gallium (Strem; purity 99.99%; or Aldrich, purity 99.9999%) was achieved from a boron nitride or tantalum cell heated to ≈1100 or ≈900 °C, respectively. The metal vapor was co-deposited with silane and an excess of argon on either a highly polished copper block or a CsI window cooled to ≈12 K by means of a closed-cycle refrigerator (Leybold LB 510 or Air Products, Model CS202). Further details of the matrix assemblies at Karlsruhe and Oxford are given elsewhere.[15,20] The proportions SiH_4/Ar lay typically between 0.1:100 and 5:100, while the rate of deposition of matrix gas was ≈2 mmol h^{-1} over a period of 0.5–1.5 h. The rate of metal deposition was determined in some experiments with the aid of a microbalance to be typically 5 μg h^{-1}. Similar experiments were carried out with SiD_4 and SiD_3H in place of SiH_4.

The following gases were used (sources in parentheses): SiH_4 (Linde, >99.99%, or Aldrich, 99.9%), SiD_4 (CDN Isotopes, 98 atom% D, or prepared by the reaction of $LiAlD_4$ with $SiCl_4$ and purified by fractional condensation in vacuo), SiD_3H (prepared by reaction of $LiAlD_4$ with $SiHCl_3$ and purified by fractional condensation in vacuo), and argon (Messer, purity 99.998%, or BOC, Research grade). Gas mixtures of argon with each of the different isotopic versions of silane were prepared by standard manometric methods.

After deposition and IR analysis of the resulting matrix, the sample was exposed for several periods to radiation of different wavelengths, and the resulting changes were again monitored by IR measurements. The photolyzing radiation issued from a medium-pressure Hg lamp (Philips LP 125) operating at 70 W or from a high-pressure Hg–Xe lamp (Spectral Energy) operating at 800 W; in each case the IR radiation was absorbed by a water filter to minimize any heating effects. Light spanning a narrow band of wavelengths was delivered via an appropriate interference filter.

IR spectra recorded at Karlsruhe were measured in reflection using a Bruker 113v spectrometer operating with either a liquid-N_2-cooled MCTB or a DTGS detector to cover the wavenumber range 4000–250 cm^{-1}; those recorded at Oxford were measured in transmission over the same range using a Nicolet Magna-IR 560 instrument with a similar choice of detectors. UV-visible spectra were recorded with 0.2 and 0.5 nm resolution for the Al/SiH_4 system at Karlsruhe with an Xe arc lamp (from Oriel), an Oriel Multispec spectrograph, and a photodiode array detector; and with the a similar resolution for the Ga/SiH_4 system at Oxford with a Perkin–Elmer–Hitachi Model 330 spectrophotometer.

Ab initio MP2 and DFT BP86 calculations on a TZVPP basis set were performed with the aid of the TURBOMOLE program package.[21] Critical point and electron density calculations were plotted on the AIM 2000 version 1.0 software.[22]

Results

The IR spectra associated with the products of the thermally and photolytically initiated reactions with silane are reported in turn for Al and Ga atoms, respectively. Progress has been tracked and products have been characterized principally with reference to the IR spectra of the Ar matrices. The identities of the products have been confirmed 1) by carrying out experiments with SiD_4 or SiD_3H in place of SiH_4, 2) by comparison with the results of appropriate quantum chemical calculations, and 3) by reference to the results of earlier experiments and to the properties of related molecules.

Aluminum: IR spectra were recorded in an experiment in which Al atoms were co-deposited with SiH_4 in an excess of Ar (SiH_4/Ar = 0.1:100) (Figure 1 and Table 1). In addition to the absorptions characteristic of free SiH_4 in these conditions,[23] the spectrum of the matrix sample recorded immediately after deposition contained five absorptions attributable to a common product (**1a**) formed spontaneously by the reaction of SiH_4 with the metal atoms in their ground elec-

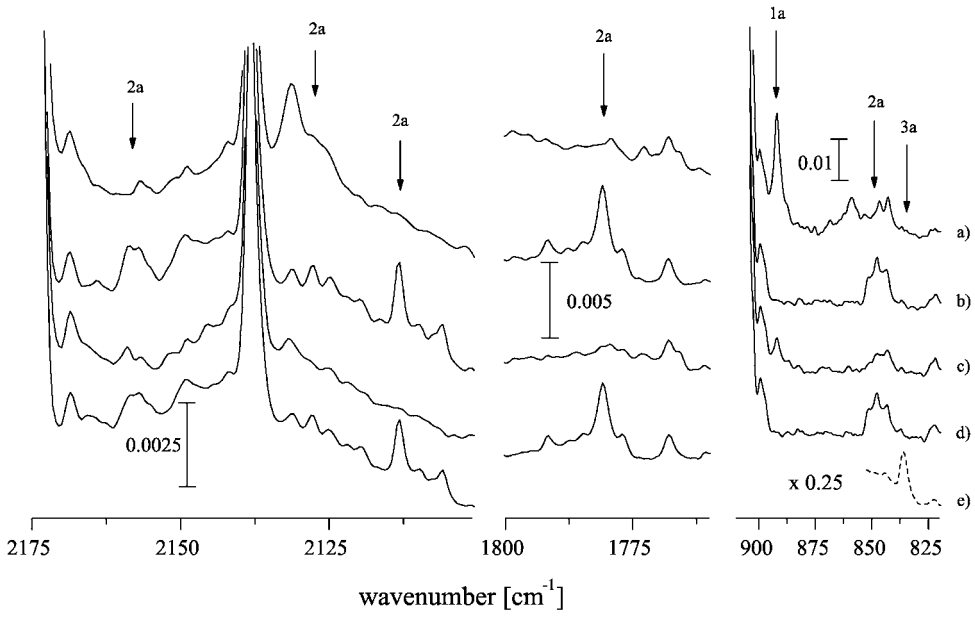

Figure 1. IR spectra showing the reactions of Al atoms with 0.1% SiH_4 in an Ar matrix: a) following deposition; b) following photolysis at $\lambda \approx 410$ nm; c) following photolysis at $\lambda \approx 580$ nm; d) following a second period of photolysis at $\lambda \approx 410$ nm. e) IR spectrum of an Ar matrix containing Al atoms and 1.5% SiH_4 following photolysis at $\lambda = 200$–800 nm.

Table 1. Observed IR wavenumbers [cm^{-1}] for the products of the reaction of Al atoms with $SiH_4/SiD_4/SiD_3H$ in a solid Ar matrix.[a]

SiH_4	SiD_4	SiD_3H	Deposition	$\lambda \approx 410$ nm	$\lambda \approx 580$ nm	$\lambda \approx 410$ nm	$\lambda \approx 200$–800 nm	Absorber
2181.1			↑	↓	↑	↓		**1a**
2174.5		2171.9	↑	↓	↑	↓		**1a**
2158.4				↑	↓	↑	↓	**2a**
2151.3							↑	**3a**
2131.4		2128.8	↑	↓	↑	↓		**1a**
2127.6				↑	↓	↑	↓	**2a**
2113.3		2109.1		↑	↓	↑	↓	**2a**
1780.9		1781.1		↑	↓	↑	↓	**2a**
	1591.1	1585.6	↑	↓	↑	↓		**1a**
	1580.5	1577.7	↑	↓	↑	↓		**1a**
	1572.9			↑	↓	↑	↓	**2a**
	1543.7			↑	↓	↑	↓	**2a**
	1520.3			↑	↓	↑	↓	**2a**
	1297.8	1297.4		↑	↓	↑	↓	**2a**
901.7		818.1	↑	↓	↑	↓		**1a**
892.4		813.8	↑	↓	↑	↓		**1a**
846.2		810.4		↑	↓	↑	↓	**2a**
836.2							↑	**3a**
	661.2	665.2	↑	↓	↑	↓		**1a**
	639.7	640.8	↑	↓	↑	↓		**1a**
	630.8	631.0		↑	↓	↑	↓	**2a**
	623.6		↑	↓	↑	↓		**1a**
	618.4						↑	**3a**

[a] ↑: increase in intensity; ↓: decrease in intensity.

tronic state. The strongest feature associated with **1a** appeared at 892.4 cm^{-1} close to the $\nu_4(t_2)$ fundamental of free SiH_4;[23] the others were located at 2181.1, 2174.5, 2131.4, 901.7, and 892.4 cm^{-1}, again in close proximity to intense SiH_4 absorptions arising from either $\nu_3(t_2)$ or $\nu_4(t_2)$. Thereafter the matrix was subjected to several cycles of selective photolysis.

Earlier matrix studies[17] had shown that the relatively sharp $^2S \leftarrow {}^2P$ absorption of Al atoms gives place to a red-shifted, broader absorption centered near 400 nm with the progressive introduction of SiH_4 to the matrix. Accordingly, we examined first the effect of irradiating the matrix sample with $\lambda \approx 410$ nm light, typically for 30 min. This caused the bands due to the initial product **1a** to decay almost to vanishing point. Simultaneously, new bands belonging to a second product **2a** developed at 2158.4, 2127.6, 2113.3, 1780.9, and 846.2 cm^{-1}. The most distinctive feature of **2a** was the strong signal at 1780.9 cm^{-1}, occurring in a region characteristic of the ν(Al–H) modes of Al^{II} species (compare $HAlNH_2$ 1761.1,[24] $HAlCH_3$ 1764/1746,[15] HAlH 1806.3/1769.5,[25] and $HAlPH_2$ 1768.2 cm^{-1}[26]). The bands at 2110–2160 and 846.2 cm^{-1} were likewise strongly suggestive of the ν(Si–H) and $\delta(SiH_3)$ modes, respectively, of an SiH_3 fragment[27] (compare $\delta(SiH_3)$ in $HHgSiH_3$ at 867.8/871.4 cm^{-1}[6]). Three of the bands due to **2a** (at 2113.3, 1780.9, and 846.2 cm^{-1}) were observed in earlier studies and attributed to the insertion product $HAlSiH_3$, which was also characterized by its UV-visible and EPR spectra.[17] The broadness of the IR bands associated with both the product and free SiH_4 and occasioned by the much higher concentrations of SiH_4 then used (SiH_4/Ar = 10:100) presumably accounts for the failure to pick out the other two ν(Si–H) features brought to light by the present experiments.

There followed a period of ≈ 30 min during which the photolyzing radiation was changed from $\lambda \approx 410$ to ≈ 580 nm. This caused the IR absorptions due to **1a** to regain some of their initial intensity at the expense of those of **2a** (Figure 1). With a second period of photolysis at $\lambda \approx 410$ nm, **1a** could be reconverted almost completely to **2a** (Figure 1d). The IR difference spectra in Figure 2 illustrate clearly this striking interconversion, which can be achieved

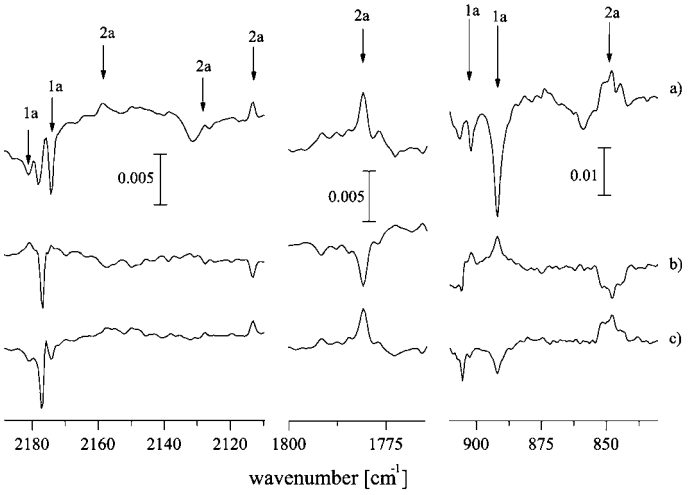

Figure 2. IR difference spectra showing the reactions of Al atoms with 0.1% SiH_4 in an Ar matrix: a) after-minus-before photolysis at $\lambda \approx$ 410 nm; b) before photolysis at $\lambda \approx 580$ nm; c) after-minus-before a second period of photolysis at $\lambda \approx 410$ nm.

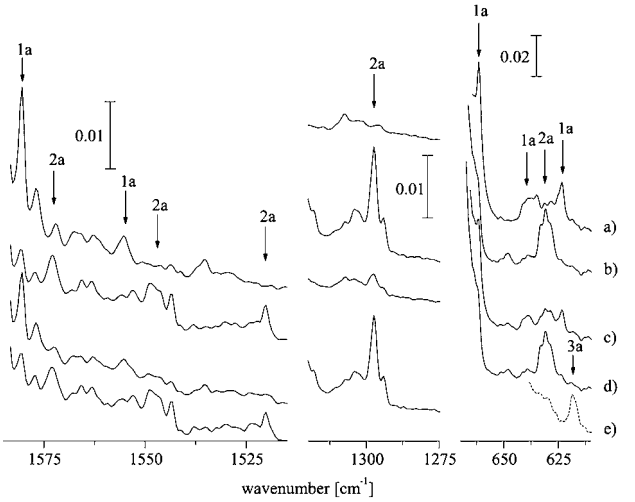

Figure 3. IR spectra showing the reactions of Al atoms with 0.3% SiD_4 in an Ar matrix: a) following deposition; b) following photolysis at $\lambda \approx$ 410 nm; c) following photolysis at $\lambda \approx 580$ nm; d) following a second period of photolysis at $\lambda \approx 410$ nm. e) IR spectrum of an Ar matrix containing Al atoms and 3.0% SiD_4 following photolysis at $\lambda = 200$–800 nm.

with near-perfect reversibility by selective photolysis. The same spectra also help to elucidate the absorptions associated with the initial product **1a**, which were invariably at risk of being masked by SiH_4 absorptions in the original spectrum.

Finally, photolysis of the matrix with broadband UV-visible light ($\lambda = 200$–800 nm) resulted in the decay of the signals due to the product **2a**, but there was no sign to suggest the regeneration of **1a**. Instead, new, weak absorptions appeared at 2151.3 and 836.2 cm^{-1}. With the wavenumbers characteristic of ν(Si–H) and $\delta(SiH_3)$ modes, respectively, these must be assigned to a third, photostable product **3a**.

In an attempt to increase the concentrations of the reaction products, and especially of **3a**, the experiments were repeated with a higher matrix concentration of SiH_4 (SiH_4/Ar = 1.5:100). Under these conditions, the absorptions of the initial product **1a** were almost completely masked by the broad and intense SiH_4 absorptions. Nevertheless, all the product bands that could be discerned had gained in intensity in comparison with their counterparts in the spectra of the more dilute matrix. The experiment thus supported our product assignments, and was particularly instructive with regard to the ultimate product of broadband UV-visible photolysis, **3a**, the two absorptions of which were now clearly visible (see Figure 1e, for example).

Additional experiments, first with SiD_4 and then with SiD_3H in place of SiH_4, were performed to investigate the products **1a**, **2a**, and **3a**. Figure 3 displays four IR spectra recorded for an Ar matrix containing 0.3% SiD_4 and one for an Ar matrix containing 3.0% SiD_4. Again, product absorptions were detectable in the spectrum recorded immediately after deposition of the dilute matrix, and could be attributed to the perdeuterated version of the product **1a**. All the features were strongly red-shifted with respect to their counterparts for the isotopically natural form of **1a**. Thus, the strong band at 623.6 cm^{-1} and the weaker one at 639.7 cm^{-1} clearly correlated with those at 892.4 and 901.7 cm^{-1} in the experiments with SiH_4 (H/D = 1.4310:1 and 1.4096:1, respectively). Likewise, the bands at 1591.1 and 1580.5 cm^{-1} were linked to those at 2181.1 and 2174.5 cm^{-1}, giving H/D ratios of 1.3708:1 and 1.3758:1, respectively. Any counterpart to the 2131.4 cm^{-1} transition of the SiH_4 product was presumably obscured by the strong absorption of free SiD_4. However, the SiD_4 product did display a band at 661.2 cm^{-1} that was not clearly matched by the SiH_4 product, again probably because of masking by other absorptions. Each of the five IR signals associated with the product **2a** was observed to shift to a substantially lower wavenumber in the SiD_4 product; the wavenumbers given in the order SiH_4 product/SiD_4 product (H/D) were: 2158.4/1572.9 (1.3722:1), 2127.6/1543.7 (1.3782:1), 2113.3/1520.3 (1.3901:1), 1780.9/1297.8 (1.3722:1), and 846.2/630.8 cm^{-1} (1.3415:1). For the perdeuterated version of **3a**, however, only one band could be detected with any certainty. Appearing at 618.4 cm^{-1}, this plainly correlated with the 836.2 cm^{-1} transition of the SiH_4 product (H/D = 1.3522:1), but the perdeutero analogue of the 2151.3 cm^{-1} transition was evidently obscured by other, stronger absorptions in the relatively congested spectral region between 1500 and 1600 cm^{-1}.

The experiments with SiD_3H followed the same pattern as those with SiH_4 and SiD_4, the only difference—but an important one—being that more, somewhat weaker IR signals were detected for the new versions of **1a** and **2a**. The spectrum of matrix-isolated SiD_3H alone showed not one but two ν(Si–H) bands, one at 2209.3 and the other at 2174.2 cm^{-1}. The higher wavenumber band broadened and decayed when the matrix temperature was raised to 20 K. The ν_3 band of SiH_4 trapped in an Ar matrix shows much the same behavior, which can be attributed to the occupation of two distinct types of defect site in the noble gas matrix.[23] The IR spectrum of the matrix containing both SiD_3H and Al atoms measured immediately after deposition now contained not five but seven new absorptions (at

2171.9, 2128.8, 1585.6, 1577.7, 818.1, 813.8, 665.2, and 640.8 cm^{-1}) belonging to the partially deuterated version (or versions) of product **1a**. Of particular note are the two features at 2171.9 and 2128.8 cm^{-1}, which must represent two distinct "isolated" ν(Si–H) modes,[19] one corresponding to an Si–H bond that is remote from the metal and the other to an Si–H bond that is coordinated to the metal. The absorptions at 1585.6 and 1577.7 cm^{-1} surely represent ν(Si–D) modes, whereas those at lower wavenumber represent deformation modes of a perturbed SiD_3H molecule. Product **2a** again gave rise to five detectable IR bands, now centered at 2109.1, 1781.1, 1297.4, 810.4, and 631.0 cm^{-1}. The first three are recognizable by their wavenumbers as originating in an "isolated" ν(Si–H), a ν(Al–H), and a ν(Al–D) mode, respectively. As in the previous experiments, the spectroscopic signs of **2a** vanished on broadband UV-visible photolysis. Unfortunately, however, the increased complexity and reduced intensity of individual product bands prevented the identification of any band clearly attributable to the product **3a** in this case, although we have no reason to doubt its formation.

UV-visible absorption spectra were also measured in order to monitor the relative abundance of Al atoms and Al_2 dimers in the matrices. With low oven temperatures (1000 °C), the spectrum of the matrix displayed only the band at 345 nm corresponding to the $^2S \leftarrow {}^2P$ transition of Al atoms;[24] the IR spectra measured under these conditions witnessed the formation of all three products **1a**, **2a**, and **3a**. Raising the oven temperature to 1100 °C gave matrices whose UV-visible spectra included not only the 345 nm band, with correspondingly enhanced intensity, but also a second, weaker band centered at 402 nm, which was identified previously[28] as arising from the Al_2 dimer. However, the IR spectra measured under these conditions differed from those measured at the lower oven temperature only in the increased intensity of all the product absorptions. Hence we infer that the species **1a**, **2a**, and **3a** are produced by the reaction of Al atoms and not Al_2 dimers or higher clusters. The UV-visible spectrum of an Ar matrix containing Al atoms and silane included a broad band at 380 nm with a full width at half maximum (FWHM) of 100 nm. This decreased after photolysis at 254 or 410 nm and regained almost its initial intensity after photolysis at 580 nm. According to its behavior and to IR spectra recorded before and after the photolysis cycles, it can be assigned to the red-shifted $^2S \leftarrow {}^2P$ transition of the Al atom in the silane complex **1a**.

Gallium: In similar experiments with Ga instead of Al vapor we expected to find close parallels between the two metals in their response to SiH_4. While such parallels certainly existed in practice, the Ga/SiH_4 system proved to be significantly more complicated and the results were accordingly more difficult to unravel. In part, this was because the IR absorptions associated with the Ga products were more prone to appear as multiplets. More seriously, the presence of the Ga_2 dimer in small but significant concentrations led to a new source of reactivity and to a product unlike any of those brought to light by the Al experiments.

Figure 4 and Table 2 detail the results of co-deposition of Ga vapor with SiH_4-doped Ar (SiH_4/Ar = 0.1:100) followed by exposure to various cycles of photolysis. On deposition, the matrix exhibited, in addition to the IR absorptions characteristic of SiH_4,[23] new features that could be shown, by their dependence on the metal concentration, to arise from not one but two products, **1b** and **4b**. The intensity of bands at 2195.8, 2178.6, 2175.3, and 903.4/901.1/897.8 cm^{-1} had a linear dependence on both metal and SiH_4 concentrations and, by analogy with the Al/SiH_4 system, are most plausibly identified with the spontaneously formed adduct **1b** of SiH_4 with Ga atoms in their ground electronic state. These contrasted with a family of bands at 2148.6, 2138.0/2128.9, 1772.0/1751.2, and 864.9 cm^{-1}, the intensities of which also varied linearly with the SiH_4 concentration, but showed a higher-order dependence on the metal concentration (see Figure 4). The most prominent and distinctive feature was

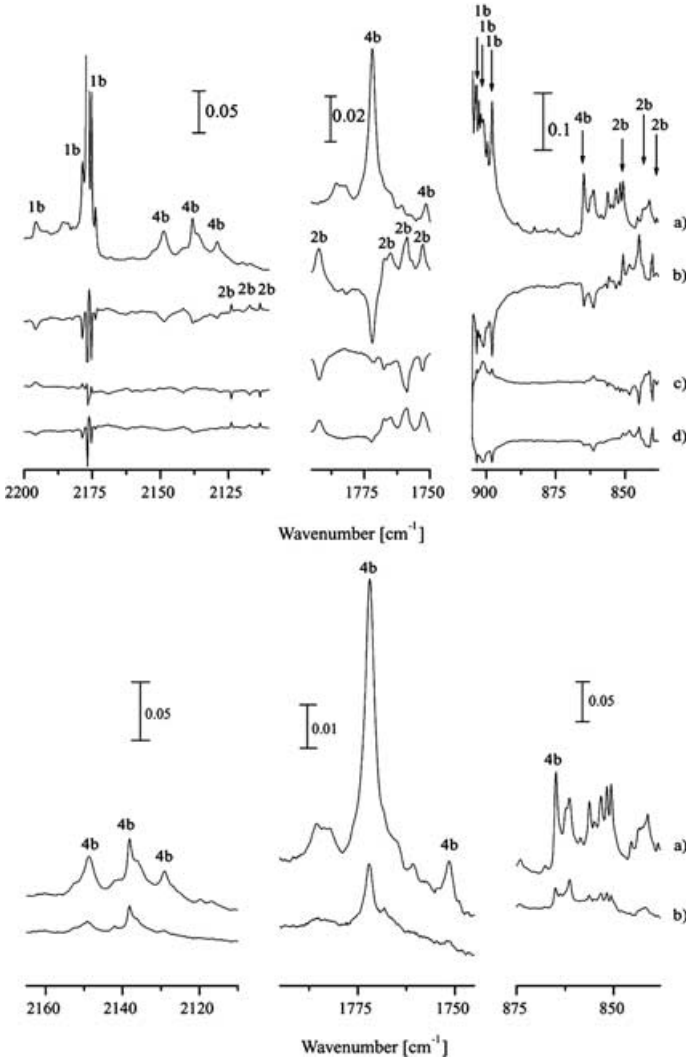

Figure 4. Top: IR spectra showing the reactions of Ga vapor with 0.1 % SiH_4 in an Ar matrix: a) following deposition; b) difference spectrum: after, minus before, photolysis at $\lambda \approx 254$ nm; c) difference spectrum: after, minus before, photolysis at $\lambda \approx 580$ nm; d) difference spectrum: after, minus before, a second photolysis at $\lambda \approx 254$ nm. Bottom: IR spectra showing the reactions of Ga vapor with 0.1 % SiH_4 in an Ar matrix with the metal oven: a) at ≈900 °C; b) at ≈850 °C.

Table 2. Observed IR wavenumbers [cm^{-1}] for the products of the reaction of Ga atoms with SiH_4 in a solid Ar matrix.[a]

SiH_4	Deposition	$\lambda\approx$ 254 nm	$\lambda\approx$ 580 nm	$\lambda\approx$ 200–800 nm	Absorber
2195.8	↑	↓	↑	↓	**1b**
2178.6	↑	↓	↑	↓	**1b**
2175.3	↑	↓	↑	↓	**1b**
2148.6	↑	↓			**4b**
2138.0	↑	↓			**4b**
2128.9	↑	↓			**4b**
2123.8		↑	↓	↓	**2b**
2117.1		↑	↓	↓	**2b**
2113.3		↑	↓	↓	**2b**
1792.1		↑	↓	↓	**2b**
1772.0	↑	↓			**4b**
1759.0		↑	↓	↓	**2b**
1752.8		↑	↓	↓	**2b**
1751.2	↑	↓			**4b**
903.4	↑	↓	↑	↓	**1b**
901.1	↑	↓	↑	↓	**1b**
897.8	↑	↓	↑	↓	**1b**
864.9	↑	↓			**4b**
848.4		↑	↓	↓	**2b**
845.0		↑	↓	↓	**2b**
840.2		↑	↓	↓	**2b**
816.2				↑	**3b**
812.9				↑	**3b**

[a] ↑: increase in intensity; ↓: decrease in intensity.

that at 1772.0 cm^{-1}, a wavenumber suggestive of the ν(Ga–H) mode of a Ga^{II} hydride;[15,24–26] at the lowest metal concentrations (achieved with oven temperatures of ≈850 °C), this was often the only clear sign of the second product, **4b**. The spectrum included other weak signals that vary in intensity from experiment to experiment and must be attributed to the products of secondary reactions between Ga atoms or Ga_2 dimers and impurities such as H_2O and H_2. Among these were bands at 1571.6, 1578.4, and 1002 cm^{-1} recognizable as belonging to the known species $Ga{\cdot}H_2O$ (A. J. Downs, V. A. Macrae, unpublished results, and ref. [29]), and $Ga(\mu\text{-}H)_2Ga$,[30] respectively. In circumstances in which $Ga_2{\cdot}H_2O$ and $Ga(\mu\text{-}H)_2Ga$ were relatively conspicuous, it was noticeable that **4b** was present in some abundance. All the signs suggest therefore that **4b** is the product of a spontaneous reaction of SiH_4, not with Ga atoms but with Ga_2 dimers.

As in the Al experiments, the matrix was then exposed to several photolysis cycles. Preliminary studies showed that irradiation at $\lambda\approx$410 nm resulted in decay of the bands due to **1b** and **4b** and the appearance of new bands. However, altogether better photoconversion and more clearcut results were achieved, particularly at low SiH_4 concentrations, by photolysis with light at $\lambda\approx$254 nm (approximating to the wavelength of the $^2D\leftarrow{}^2P$ transition of matrix-isolated Ga atoms[31]). This brought about the growth of seven new bands at 2123.8, 2117.1, 2113.3, 1792.1, 1759.0, 1752.8, and 848.4/845.0/840.2 cm^{-1} associated with a product **2b**. The strongest feature, near 845.0 cm^{-1}, occurs in the region characteristic of $\delta(SiH_3)$ vibrational modes,[27] whereas the multiplet at 1792.1/1759.0/1752.8 cm^{-1} is likely to represent a ν(Ga–H) mode of a divalent Ga species (compare $HGaNH_2$ 1721.8,[24] $HGaCH_3$ 1719.7,[15] HGaH 1806.3/1769.5,[25] and $HGaPH_2$ 1768.2 cm^{-1}[26]). All the signs are that **2b** is the Ga analogue of the Al species **2a**.

Thereafter the matrix was subjected to a second photolysis cycle with $\lambda\approx$580 nm light. This led to the re-appearance of the bands due to the initial product **1b** (but not of **4b**) and the simultaneous decay of the bands due to **2b**. A last photolysis cycle with broadband radiation (λ = 200–800 nm) led to the decay of the absorptions of **1b** and a further decay of those due to **2b**. At the same time, a new feature grew in at 816.2/812.9 cm^{-1} in a region characteristic of $\delta(SiH_3)$ vibrational modes.[27] The absorber responsible for this band is most likely to be the Ga analogue, **3b**, of the species **3a** formed in the corresponding experiments with Al.

The experiment was repeated using SiD_4 instead of SiH_4 to assess the response of the matrices to photolysis cycles that followed the same pattern as with SiH_4. In the case of SiD_4, absorptions at 1559.4, 1536.9, and 666.1 cm^{-1} attributable to product **1b** were detected. The red shift of the most distinct absorption (at 666.1 cm^{-1}) relative to the corresponding feature of the SiH_4 product at 897.8 cm^{-1} gives an H/D ratio of 1.3478:1. The other bands arising from the SiD_4 product were both recognizable as having counterparts in the spectrum of the SiH_4 product, as attested by the relevant H/D ratios. The deuterated version of **4b** was recognizable by bands at 1571.5 and 1277.3 cm^{-1}, the latter being the more intense and plainly correlating with the 1772.0 cm^{-1} transition of the ^1H product so that H/D = 1.3873:1. Following photolysis at $\lambda\approx$254 nm, new bands attributable to **2b** in its perdeuterated form appeared at 1292.5/1269.2 and 629.3 cm^{-1}; correlation with analogous features of the normal form gives H/D ratios of 1.3865/1.3859:1 and 1.3428:1, respectively. No absorptions attributable to product **3b** in its perdeuterated form could be observed.

Unfortunately, the combination of low intensity and multiplet structure that characterized the product bands frustrated attempts to add significantly to the information available from experiments with SiD_3H. Some of the expected bands were certainly observed, but it was not possible to locate with any confidence "isolated" ν(Si–H) modes for either **1b** or **2b**.

UV-visible absorption spectra of the matrices were also measured. With low oven temperatures (850 °C), the 300–900 nm range of the spectrum of an Ar matrix containing Ga and a low concentration of SiH_4 displayed only a sharp UV band at 342 nm, corresponding to the $^2S\leftarrow{}^2P$ transition of atomic Ga;[31] the IR spectra measured under these conditions, followed by the appropriate photolysis cycles, witnessed the formation of all four products **1b**, **2b**, **3b**, and **4b**. Raising the oven temperature gave matrices whose UV-visible spectrum included not only the 342 nm band, with correspondingly enhanced intensity, but also a second absorption, much weaker and broader than the first. Centered at 610 nm, this was identified previously[28] as arising from the Ga_2 dimer. As in the case of the Al/SiH_4 system, the IR spectra measured under these conditions differed from those measured at the lower oven temperature only in the increased intensity of all the product absorptions, but particularly of those due to **4b**, lending confidence to the view

that **1b**, **2b**, and **3b** are monometal products, whereas **4b** is a dimetal product. As the initial concentration of SiH_4 in the matrix increased, the sharp band at 342 nm gradually gave place to a much broader one at somewhat longer wavelength. With a matrix ratio $SiH_4/Ar = 5:100$, no trace was evident of the 342 nm transition, which had been replaced by an absorption with an FWHM of 90 nm centered near 350 nm. Irradiation of the matrix at $\lambda \approx 254$ nm caused this feature to decay almost to vanishing point. Although no new absorption could be perceived to develop, exposure of the matrix to 580 nm light was then found to restore the 350 nm band, only for this to be extinguished by subsequent exposure to broadband UV-visible light. From its behavior, the 350 nm feature must be associated with the product **1b**, so presumably it represents the counterpart to the 380 nm band attributable to the Al species **1a**. Although its diffuseness meant that there was still significant absorption at $\approx$410 nm, the poorer wavelength match of photolyzing radiation to maximum UV absorption was plainly responsible for the reduced efficiency of 410 nm photolysis in the Ga case.

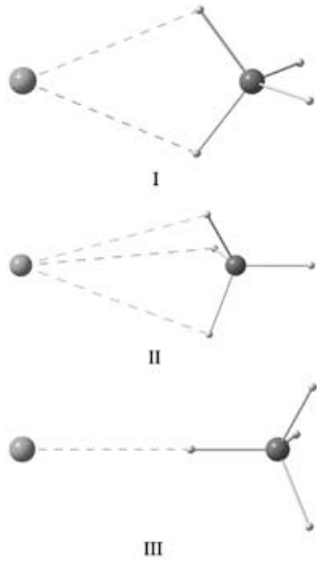

Figure 5. Calculated structures of the three possible isomers of $M{\cdot}SiH_4$ (M = Al or Ga) with M approaching an edge (**I**), a face (**II**), and a corner (**III**) of the SiH_4 tetrahedron.

Discussion

Combination of all the results derived both from experiment and from detailed quantum chemical calculations leads us to identify the products as, successively, the complex $M{\cdot}SiH_4$ (**1a**, **1b**), its tautomer $HMSiH_3$ (**2a**, **2b**), from which it can be regenerated photolytically [Eq. (1)], and the simple M^I species $MSiH_3$ (**3a**, **3b**), where M = Al or Ga. The experiments with Ga vapor give evidence of spontaneous insertion into an Si–H bond by the Ga_2 dimer, probably to form the unprecedented SiH_3-bridged digallium hydride $HGa(\mu\text{-}SiH_3)Ga$ (**4b**) [Eq. (2)].

$$M \cdots SiH_4 \underset{\lambda \approx 580\,nm}{\overset{\lambda \approx 254 \text{ or } 410\,nm}{\rightleftharpoons}} HM{\cdot}SiH_3 \qquad (1)$$

$$Ga_2\,(^3\Pi) + SiH_4 \longrightarrow \begin{array}{c} H_3 \\ H \quad Si \\ Ga\!-\!Ga \end{array} \qquad (2)$$

$M{\cdot}SiH_4$ [M = Al (1a) or Ga (1b)]: The IR signatures observed for the products **1a** and **1b** are all very close to the absorptions of free SiH_4. This, allied to the conditions of formation and the precedents of earlier studies,[24,26] suggests that **1a** and **1b** each contain a perturbed SiH_4 group. The prime candidate is a complex of the form $M{\cdot}SiH_4$. For such a complex, there are three possible geometries (Figure 5). Structure **I** features an M atom located above the midpoint of one of the edges of the SiH_4 tetrahedron, resulting in a geometry with C_{2v} symmetry. In **II** the M atom is located above one of the four faces, and in **III** it is near one of the corners of the SiH_4 tetrahedron; in both the assembly conforms to C_{3v} symmetry. The optimized dimensions of the three possible structures, as derived from ab initio MP2 and DFT BP86 calculations, are given in Table 3 for M = Al and M = Ga. Hereafter the results of these calculations are given in the order MP2/BP86. Hence **I** represents the global minimum structure for both M = Al and M = Ga, whereas **II** and **III** have minima lying, 2.1/6.2 and 3.9/10.7 kJ mol^{-1}, respectively, to higher energy for M = Al, and 6.1/10.8 and 3.6/6.6 kJ mol^{-1}, respectively, to higher energy for M = Ga. The reaction of Al atoms with SiH_4 to give the adduct $Al{\cdot}SiH_4$ in its global minimum C_{2v} structure is exothermic by $-5.4/-12.0$ kJ mol^{-1}; that of Ga atoms to give $Ga{\cdot}SiH_4$ is similarly exothermic by $-8.8/-12.5$ kJ mol^{-1}. For M = Al, the best match of the experimental with the calculated wavenumbers (Table 4) is achieved for the C_{2v} structure **I** (that is, with the Al atom located above an edge of the SiH_4 tetrahedron), in agreement with the calculated energies of the different conformers (see Supporting Information). In effect, the preferred form involves η^2 coordination of the SiH_4. The observed pattern of a doublet to high wavenumber and a singlet to low wavenumber is identical with that characterizing an η^2-coordinated BH_4^- ligand[32] as found, for example, in $H_2Ga(\mu\text{-}H)_2BH_2$.[33]

As evidenced by the matrix site effects noted here and in earlier matrix[23] and other studies,[34] the ν(Si–H) fundamentals of silane are particularly sensitive reporters of environment. Accordingly, their wavenumbers carry additional information about the $M{\cdot}SiH_4$ complexes. The calculations indicate that two ν(Si–H) modes of $M{\cdot}SiH_4$ are red-shifted, and the other two blue-shifted with respect to the antisymmetric ν(Si–H) fundamental, $\nu_3(t_2)$, of free SiH_4; the three IR absorptions that can be perceived in this region for both M = Al and M = Ga are consistent with this pattern (Tables 4 and 5). We infer that the Si–H bonds directed toward the metal are elongated, whereas the Si–H bonds pointing away from the metal are shortened, either because there is a slight transfer of charge in the direction $SiH_4 \rightarrow M$ or as a result of polarization effects. Any charge transfer must, however, be much smaller than in the corresponding Al or Ga complex of the much more basic NH_3 molecule,

Table 3. Calculated dimensions of the three possible isomers of M·SiH_4, with the M atom approaching an edge (**I**), a face (**II**), and a corner (**III**) of the SiH_4 tetrahedron, and of $HMSiH_3$ and $MSiH_3$.

	M·SiH_4 (**I**)		M·SiH_4 (**II**)		M·SiH_4 (**III**)		$HMSiH_3$		$MSiH_3$	
	MP2	BP	MP2	BP	MP2	BP	MP2	BP	MP2	BP
M = Al										
energy [kJ mol^{-1}][a]	−5.4	−12.0	−3.3	−5.8	−1.5	−1.3	−59.0	−68.7		
r(Al···Si) [pm]	368.7	304.4	420.4	441.1	435.1	382.8	248.4	249.4	259.3	260.8
r(Si–H) [pm]	147.6/148.0[b]	149.5/150.5[b]	147.6/147.8[b]	149.8/149.3[b]	147.6/148.1[b]	149.13/151.14[b]	148.5/148.2	150.3/149.8	149.0	150.9
r(Al···SiH_4) [pm]	469.1/306.2	409.3/243.6	395.6/568.1	416.9/590.9	502.9/287.0	452.6/231.6				
r(H-Al-SiH_3) [pm]							159.4	161.9		
∢(Al-Si-H) [°]	124.9/54.0	125.2/52.4	180.0/70.2	180.0/70.9	109.0/0.0	108.0/0.0	112.3/110.8	112.8/110.9	112.7	113.4
∢(H-Al-SiH_3) [°]							118.3	117.7		
M = Ga										
energy [kJ mol^{-1}][a]	−8.8	−12.5	−2.7	−1.7	−5.2	−5.9	−34.0	−30.4		
r(Ga···Si) [pm]	344.4	308.6	397.3	432.4	410.8	382.4	243.2	246.9	257.8	260.9
r(Si–H) [pm]	147.6/148.2[b]	149.5/150.3[b]	147.6/147.8[b]	149.9/149.3[b]	147.6/148.2[b]	149.2/150.7	148.4/147.9	150.2/149.6	149.0	150.9
r(Ga···SiH_4) [pm]	445.5/283.4	413.4/249.3	374.3/544.9	409.0/582.3	479.5/262.6	452.5/231.7				
r(H-Ga-SiH_3) [pm]							157.0	160.9		
∢(Ga-Si-H) [°]	124.9/53.8	125.3/53.1	180.0/70.0	180.0/71.0	108.8/0.0	108.5/0.0	111.6/110.3	111.7/110.6	112.6	113.4
∢(H-Ga-SiH_3) [°]							121.6	120.5		

[a] Relative to free M and SiH_4 in their ground electronic states. [b] H atoms pointing toward the M atom.

Table 4. Experimental IR wavenumbers [cm^{-1}] of Al·SiH_4 and calculated wavenumbers [cm^{-1}] and intensities [km mol^{-1}, given in parentheses] of the three isomers **I**, **II**, and **III**.

Obsd	Assign	**I**		**II**		**III**	
		BP	MP2	BP	MP2	BP	MP2
2181.1	$\nu_1(a_1)$	2173.4 (253)	2311.8 (132)	2209.6 (67)	2318.4 (99)	2187.1 (97)	2313.6 (138)
2174.5	$\nu_7(b_1)$	2172.8 (72)	2318.3 (94)	2206.4 (64)	2317.0 (100)	2184.7 (100)	2309.2 (88)
2131.4	$\nu_2(a_1)$	2125.1 (50)	2283.0 (87)	2159.3 (64)	2307.4 (56)	2172.1 (122)	2305.4 (95)
	$\nu_{10}(b_2)$	2124.6 (18)	2283.8 (76)	2064.0 (295)	2274.5 (236)	2149.6 (257)	2298.5 (9)
	$\nu_3(a_1)$	928.4 (44)	1001.9 (1)	934.7 (1)	1002.7 (0.1)	931.4 (0.3)	1006.1 (0.4)
901.7	$\nu_{11}(b_2)$	878.7 (58)	950.7 (114)	921.3 (20)	998.4 (1)	928.7 (0.4)	1003.3 (0.1)
892.4	$\nu_4(a_1)$	869.2 (320)	943.9 (288)	877.5 (134)	949.9 (139)	869.4 (96)	949.2 (143)
	$\nu_6(a_2)$	826.1 (0)	991.4 (0)	875.5 (185)	944.8 (225)	854.6 (144)	948.3 (128)
	$\nu_8(b_1)$	748.2 (34)	934.6 (117)	821.3 (44)	943.1 (132)	848.1 (162)	946.9 (190)
	$\nu_{12}(b_2)$	343.9 (2)	150.8 (0.4)	284.8 (0.1)	172.4 (0.2)	111.0 (0.1)	110.2 (0.1)
	$\nu_9(b_1)$	282.4 (0.1)	151.5 (0.1)	260.5 (0.2)	163.2 (0.1)	52.0 (2)	86.0 (0.1)
	$\nu_5(a_1)$	137.2 (5)	54.4 (2)	105.8 (3)	46.9 (1)	30.1 (1)	34.5 (0.1)

Table 5. Experimental IR wavenumbers [cm^{-1}] of Ga·SiH_4 and calculated wavenumbers [cm^{-1}] and intensities [km mol^{-1}, given in parentheses] of the three isomers **I**, **II**, and **III**.

Obsd	Assign	**I**		**II**		**III**	
		BP	MP2	BP	MP2	BP	MP2
2195.8	$\nu_1(a_1)$	2173.76 (229)	2312.76 (139)	2192.52 (86)	2314.58 (134)	2211.09 (66)	2318.91 (100)
2178.6	$\nu_7(b_1)$	2173.27 (78)	2320.11 (92)	2181.55 (102)	2307.72 (86)	2206.99 (65)	2318.50 (99)
2175.3	$\nu_2(b_2)$	2133.57 (31)	2278.51 (69)	2179.94 (79)	2304.22 (94)	2093.05 (363)	2307.91 (54)
	$\nu_{10}(a_1)$	2132.19 (46)	2276.94 (86)	2147.36 (206)	2304.22 (11)	2072.01 (4)	2268.54 (270)
903.4/901.1/897.8	$\nu_3(a_1)$	929.57 (26)	1004.35 (0.1)	929.75 (0.3)	1005.73 (0.5)	935.72 (3)	1000.50 (0.2)
	$\nu_{11}(b_2)$	877.03 (65)	955.82 (113)	927.05 (1)	1003.39 (0.4)	916.90 (21)	994.18 (5)
	$\nu_4(a_1)$	870.51 (314)	946.57 (307)	870.37 (96)	948.53 (136)	873.09 (95)	948.00 (139)
	$\nu_6(a_2)$	830.39 (0)	989.06 (0)	860.01 (121)	947.54 (136)	867.54 (224)	942.63 (241)
	$\nu_8(b_1)$	744.23 (42)	929.43 (109)	839.44 (200)	946.01 (188)	810.16 (45)	935.70 (124)
	$\nu_{12}(b_2)$	286.78 (1)	179.21 (0.5)	135.27 (0.6)	117.47 (0.08)	220.32 (0.23)	135.49 (0.02)
	$\nu_9(b_1)$	184.27 (0.8)	177.24 (0.04)	120.69 (0.06)	92.59 (0.08)	165.25 (0.06)	128.57 (0.03)
	$\nu_5(a_1)$	106.97 (1)	48.75 (1)	21.66 (0.7)	32.12 (0.1)	84.38 (1)	48.93 (1)

where it was clearly evidenced by the IR,[24,35] UV-visible,[24] and EPR[35,36] spectra.

Of particular note are the ν(Si–H) bands associated with the partially deuterated species M·SiD$_3$H. For SiD$_3$H isolated alone in what seems to be its primary, stable site in a solid Ar matrix at $\approx$12 K, the relevant band occurs at 2174.2 cm^{-1}. It is therefore red-shifted by 13.0 cm^{-1} with respect to the gaseous molecule,[19] in keeping with the exercise of a purely dielectric effect of the matrix on a relatively polarizable molecule. No similar band or bands could be observed for the complex Ga·SiD$_3$H, but Al·SiD$_3$H was found to give rise to two ν(Si–H) bands, both shifted to low wavenumber of the corresponding mode of the parent SiD$_3$H. The two distinct "isolated" Si–H stretching modes, ν^{is}(Si–H),[19] thus identified clearly relate to two types of Si–H bond, one stronger than the other, with the added advantage of eliminating any doubts about the possible effects of vibrational coupling of ν(Si–H) modes or of Fermi resonance.[19] The relevant bands could be discerned weakly but clearly only in difference spectra following photolysis at $\lambda \approx 410$ nm, and notwithstanding the difficulties of estimating intensities reliably under these circumstances, they appeared to be of comparable intensity. This is consistent with the presence of strong and weak Si–H bonds in equal numbers, as required only by model **I** (compare **II** and **III**). For a limited range of silanes that includes SiH$_4$, McKean and co-workers[19] have established a correlation between ν^{is}(Si–H) and r_0(Si–H) that takes the simple linear form of Equation (3). Although

$$r_0(\text{Si–H})\ [\text{pm}] = 187.29 - 0.01798\nu^{is}(\text{Si–H})\ [\text{cm}^{-1}] \quad (3)$$

this is somewhat lower in scope and reliability than an analogous relation linking ν^{is}(C–H) to r_0(C–H),[37] its predictive capability in relation to r_0 values is reported to be better than $\pm$0.3 pm, at least for silane derivatives with fully saturated bonding. Where specific interactions create differences between the Si–H bonds in a particular molecule, Equation (3) may be expected to provide a reasonably faithful estimate of the *difference* in bond length, Δr_0(Si–H). On this basis, Δr_0(Si–H) is 0.77 pm for Al·SiH$_4$.

Using ab initio calculations with a 4-21G/3-3-21G basis set, McKean and co-workers[19] have determined r_e(Si–H) distances for various silanes and shown that these too correlate well with experimentally determined ν^{is}(Si–H) values in accordance with Equation (4). Hence we calculate Δr_e(Si–H) = 0.86 pm for Al·SiH$_4$. The empirical approaches embodied in Equations (3) and (4) thus give results in satisfactory agreement with regard both the absolute Si–H distances and the difference between them, with those of our MP2 and DFT calculations (see Table 3). Coordination of the SiH$_4$ molecule is calculated to cause the Si–H bonds directed toward the metal to be attenuated by 0.4–1.0 pm relative to the bonds directed away from the metal. The degree of perturbation of the SiH$_4$ thus implied is small but comparable in magnitude with that often experienced by a CH$_n$ or SiH$_n$ unit which is coordinated to a transition-metal center and subject to a weak secondary or "agostic" interaction with the metal.[1,38] Such interactions may be critical in prefiguring potential reaction pathways.

$$r_e(\text{Si–H})\ [\text{pm}] = 190.89 - 0.01998\nu^{is}(\text{Si–H})\ [\text{cm}^{-1}] \quad (4)$$

Figure 6 (top) shows an electron density distribution plot of the Al·SiH$_4$ complex, including the bond critical points.[22]

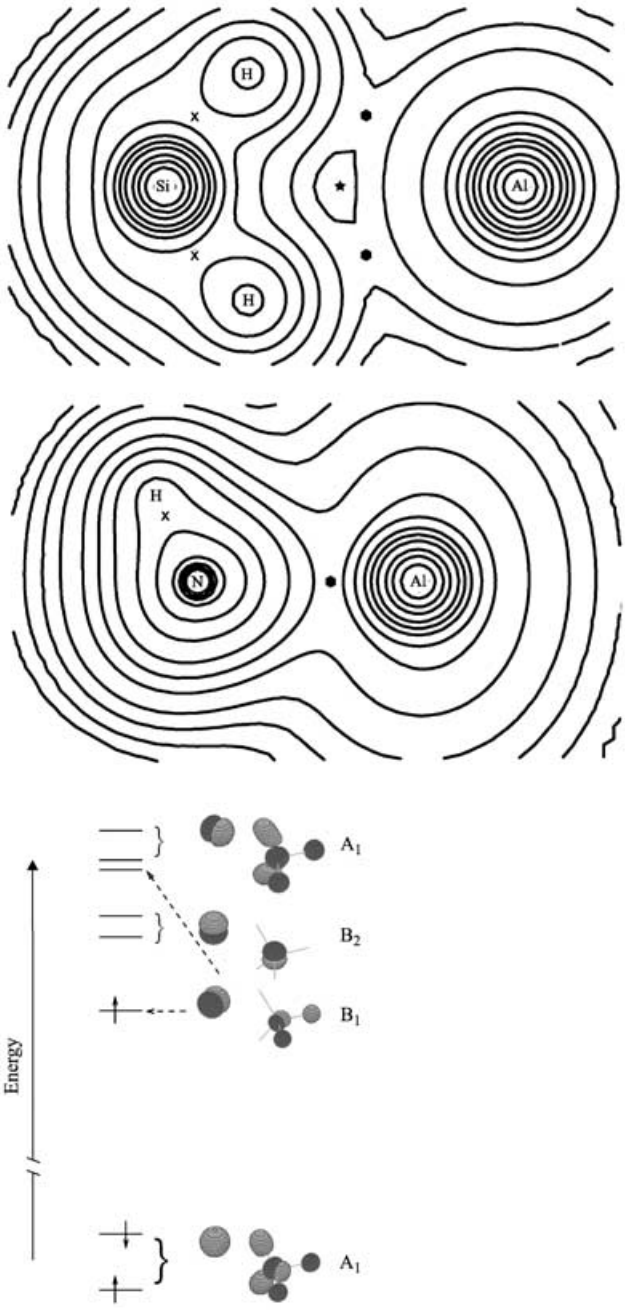

Figure 6. Top: The electron density distribution in Al·SiH$_4$ and Al·NH$_3$ (contour values [e pm^{-3}]: 4×10^{-1}, 2×10^{-1}, 8×10^{-2}, 4×10^{-2}, 2×10^{-2}, 8×10^{-3}, 4×10^{-3}, 2×10^{-3}, 8×10^{-4}, 4×10^{-4}, 2×10^{-4}, 8×10^{-5}, 4×10^{-5}) and the bond critical points. Saddle points: × (68.3×10^{-9} e pm^{-3} for the Si–H bond in Al·SiH$_4$ directed toward the Al atom; 32.3×10^{-9} e pm^{-3} (Al·SiH$_4$) and 340.8×10^{-9}/342.9×10^{-9} e pm^{-3} (Al·NH$_3$) for the Si–H and N–H bonds directed away from the Al atom) and ● (4.5×10^{-9} e pm^{-3}, and 3.3×10^{-9} e pm^{-3} for Al·SiH$_4$ and Al·NH$_3$, respectively). Local minimum of the electron density: ★ (3.0×10^{-9} e pm^{-3} for Al·SiH$_4$). Bottom: The MO scheme and the shapes of the frontier orbitals (α and β spin orbitals) for Al·SiH$_4$.

Hence it is clear that the bonding between Al and SiH_4 occurs through the H atoms and not directly between the Al and Si atoms. Nevertheless, the electron density between the Al and H atoms, at 4.54×10^{-9} e pm^{-3}, is significantly lower than that between Al and N atoms in the more strongly bonded Al·NH_3 complex (32.83×10^{-9} e pm^{-3}). Finally, the frontier orbitals were evaluated (Figure 6, bottom). They can be described as weakly perturbed Al and SiH_4 orbitals with relatively little overlap, in keeping with the experimental results.

We have performed similar calculations for a complex Al·CH_4, despite the absence of experimental data in this case. The energy for the formation of this complex starting from CH_4 and an Al atom in its ground electronic state is about -2.6 kJ mol^{-1}, that is, 2.8 kJ mol^{-1} lower than for the Al·SiH_4 complex (at the MP2 level). The Al···C distance is some 30 pm longer than the Al···Si distance in the corresponding SiH_4 complex (see Supporting Information). As a consequence of the very weak perturbation of the CH_4 molecule by the Al atom, the vibrational modes suffer only small changes of wavenumber. It is not altogether surprising, therefore, that the Al·CH_4 complex has so far eluded detection, although it is presumably present in Ar matrices formed by co-condensing Al vapor with CH_4 and is the precursor to the photochemical activation of the CH_4 molecule which can be brought about under these conditions.[15,16]

$HMSiH_3$ [M = Al (2a) or Ga (2b)]: The IR spectroscopic results collected for the various isotopomers of the products **2a** and **2b** indicate that each hosts a terminal M–H bond and an SiH_3 group. The clear inference is that insertion of the metal atom into an Si–H bond of SiH_4 has taken place to afford $HMSiH_3$, that is, an M^{II} derivative. Strong circumstantial support for such an assignment comes from earlier studies which show that a photoactivated Al or Ga atom in its ^{2}S or ^{2}D excited state, and within the confines of a matrix, is capable of inserting into various bonds, engaging hydrogen with either itself or another atom (for example, in H_2,[25] CH_4,[15,16] NH_3,[24] or H_2O.[29]) According to our DFT calculations, $HAlSiH_3$ and $HGaSiH_3$ each has a global minimum structure with C_s symmetry. $HAlSiH_3$ is characterized by Al–Si, Al–H and Si–H distances of 248.4, 159.4, and 148.5/148.2 pm, respectively, and an Si-Al-H angle of 118.3°; in the case of $HGaSiH_3$, the Ga–Si, Ga–H, and Si–H distances are 243.2, 157.0, and 148.4/147.9 pm, respectively, and the Si-Ga-H angle is 121.6° (see Table 3). Experiments and calculations agree that the $HMSiH_3$ molecules do not contain a hydrogen bridge, as one might have expected, but they do favor a structure closely resembling that of $HMCH_3$,[15,16] with the unpaired electron located near the metal atom. The calculated wavenumbers and IR intensities for the vibrational fundamentals of the four isotopomers $HMSiH_3$, $DMSiD_3$, $HMSiD_3$, and $DMSiD_2H$ detected in our experiments are in satisfactory agreement with the observed features (see Tables 6 and 7 for M = Al and Ga, respectively), when due allowance is made for details lost either for want of intensity or through masking by stronger absorptions due to other species. The appearance of not one but three bands for $HGaSiH_3$ in the region 1700–1800 cm^{-1} must be ascribed to Fermi resonance involving the ν(Ga–H) fundamental and either the combination $\nu_4+\nu_5$ or the overtone $2\nu_{10}$ (setting both ν_4 and ν_{10} near 900 cm^{-1}).

The IR spectra measured for the $HMSiH_3$, $DMSiD_3$, $HMSiD_3$, and $DMSiD_2H$ molecules do not in themselves

Table 7. Observed and calculated IR wavenumbers [cm^{-1}] and calculated intensities [km mol^{-1}, given in parentheses] for $HGaSiH_3$ and $DGaSiD_3$.

$HGaSiH_3$		$DGaSiD_3$		Assign
obsd	calcd[a]	obsd	calcd[a]	
–[b]	2166.9 (82)	–[b]	1563.9 (46)	ν_1(a′)
2123.8	2147.2 (69)	–[b]	1514.9 (31)	ν_2(a′)
1792.1/1759.0/1752.8	1732.9 (276)	1292.5/1269.2	1234.9 (140)	ν_3(a′)
–[b]	915.0 (31)	–[b]	642.3 (20)	ν_4(a′)
848.8/845.0/840.2	814.3 (263)	629.3	601.7 (133)	ν_5(a′)
–[b]	551.7 (24)	–[b]	409.1 (11)	ν_6(a′)
–[b]	367.5 (18)	–[b]	271.9 (9)	ν_7(a′)
–[b]	349.9 (15)	–[b]	260.1 (7)	ν_8(a′)
2117.1/2113.3	2126.6 (55)	–[b]	1551.4 (40)	ν_9(a″)
–[b]	897.2 (36)	–[b]	656.1 (17)	ν_{10}(a″)
–[b]	280.0 (4)	–[b]	254.2 (8)	ν_{11}(a″)
–[b]	191.3 (1)	–[b]	137.6 (1)	ν_{12}(a″)

[a] DFT calculation using the BP86 method and a TZVPP-type basis set. [b] Too weak to be observed, or obscured.

Table 6. Observed and calculated IR wavenumbers [cm^{-1}] and calculated intensities [km mol^{-1}, given in parentheses] for $HAlSiH_3$, $DAlSiD_3$, $HAlSiD_3$, and $DAlSiD_2H$ in C_s or C_1 symmetry.

$HAlSiH_3$		$DAlSiD_3$		$HAlSiD_3$		$DAlSiD_2H$ (C_s)		$DAlSiHD_2$ (C_1)	Assignment
obsd	calcd[a]	obsd	calcd[a]	obsd	calcd[a]	obsd	calcd[a]	calcd[a]	
2158.4	2161.9 (79)	1572.9	1559.7 (44)	1781.1	1780.3 (223)	2109.1	2160.5 (77)	2134.3 (67)	ν_1(a′)
2113.3	2126.7 (57)	1520.3	1515.8 (31)	–[b]	1559.7 (42)	–[b]	1522.4 (32)	1529.4 (34)	ν_2(a′)
1780.9	1780.2 (220)	1297.8	1282.2 (116)	–[b]	1515.8 (33)	1297.4	1282.2 (115)	1283.0 (115)	ν_3(a′)
–[b]	904.9 (32)	–[b]	647.4 (18)	–[b]	647.5 (19)	–[b]	763.3 (98)	748.7 (104)	ν_4(a′)
846.2	836.5 (221)	630.8	618.1 (107)	631.0	618.5 (98)	–[b]	633.2 (48)	644.3 (64)	ν_5(a′)
–[b]	575.5 (48)	–[b]	431.0 (31)	–[b]	538.6 (73)	–[b]	454.1 (34)	443.5 (19)	ν_6(a′)
–[b]	412.9 (31)	–[b]	344.2 (11)	–[b]	345.5 (11)	–[b]	360.8 (21)	349.4 (6)	ν_7(a′)
–[b]	345.8 (3)	–[b]	287.4 (10)	–[b]	315.8 (6)	–[b]	299.0 (9)	293.1 (10)	ν_8(a′)
2127.6	2139.7 (71)	1543.7	1545.4 (40)	–[b]	1545.4 (40)	–[b]	1545.4 (40)	1559.2 (42)	ν_9(a″)
–[b]	919.1 (28)	–[b]	658.4 (15)	–[b]	658.4 (15)	810.4	823.8 (28)	809.7 (29)	ν_{10}(a″)
–[b]	425.1 (16)	–[b]	308.4 (7)	–[b]	307.9 (6)	–[b]	318.1 (7)	342.9 (20)	ν_{11}(a″)
–[b]	331.4 (9)	–[b]	239.7 (5)	–[b]	335.4 (14)	–[b]	240.0 (4)	220.4 (4)	ν_{12}(a″)

[a] DFT calculation using the BP86 method and a TZVPP-type basis set. [b] Too weak to be observed, or obscured.

give any direct guidance to the geometry of the molecules. However, the ν^{is}(Si–H) mode of the isotopomer $DAlSiD_2H$ has been located at 2109.1 cm^{-1}. On the assumption that Equations (3) and (4) are applicable, the ν^{is}(Si–H) wavenumbers translate into the Si–H bond lengths $r_0 = 149.4$ pm, $r_e = 148.8$ pm. As predicted by the MP2 and DFT calculations (Table 3), these distances are about 1–2 pm longer than in free SiH_4, and slightly longer even than the more attenuated of the Si–H bonds in the Al·SiH_4 adduct. Although this may suggest a small contribution of antibonding Si–H to the makeup of the molecular orbital occupied by the unpaired electron, a more significant factor is likely to be the partial negative charge that the SiH_3 group assumes when linked to the electropositive metal atom. Unfortunately the ν^{is}(Si–H) mode of the isotopomer $DGaSiD_2H$ could not be observed.

$MSiH_3$ [M = Al (3a) or Ga (3b)]: As already noted, the IR signals near 2150 and 840 cm^{-1} associated with the product **3a**, as formed from SiH_4, are most plausibly assigned to ν(Si–H) and $\delta(SiH_3)$ vibrations, respectively. Product **3b** could be identified only by a signal near 815 cm^{-1}. Hence these products are likely to contain an SiH_n moiety, but there is no longer any sign of an M–H bond. Disilane, Si_2H_6, is a known secondary product of similar matrix reactions involving a Group 12 metal atom such as Zn.[6,39] The possibility that this or the $SiH_3^{\bullet}$ radical is being formed by the present reactions can be largely discounted by comparison with the spectra recorded previously for these species under matrix conditions.[6,40] The precedents of earlier matrix studies are that divalent aluminum or gallium hydrides, such as HMOH,[29] $HMNH_2$,[24] $HMCH_3$,[15,16] and HMH,[25] are photolabile and decompose under the action of broadband UV-visible irradiation through cleavage of the M–H bond to form the appropriate M^I compound and $H^{\bullet}$ atoms. Accordingly, the ultimate photoproducts **3a** and **3b** are most probably the M^I species $AlSiH_3$ and $GaSiH_3$, respectively. DFT calculations find a global minimum energy that corresponds to a geometry conforming to C_{3v} symmetry. The distances and angles are: $AlSiH_3$, r(Al–Si) 259.3 pm, r(Si–H) 149.0 pm, ∢H-Si-Al 112.7°; $GaSiH_3$, r(Ga–Si) 257.8 pm, r(Si–H) 149.0 pm, ∢H-Si-Ga 112.6°. Comparison of the IR properties simulated for the normal and perdeuterated forms of the two molecules (see Supporting Information) with the limited experimental data attributable to **3a** and **3b** shows that the transitions expected to be most intense in IR absorption are matched by experiment, with wavenumbers in pleasing agreement with the calculated ones. Despite the sparseness of the experimental evidence, we have no reason to doubt that $HMSiH_3$ emulates $HMCH_3$[15,16] in its response to broadband UV-visible light, and that its decomposition gives rise to $H^{\bullet} + MSiH_3$.

HGa(μ-SiH_3)Ga (4b): The product **4b** is formed on co-deposition of Ga vapor with SiH_4 in yields that vary with the metal concentration so as to suggest that Ga_2 and SiH_4 are its sources. There is a clear analogy with observations on co-deposition of Ga vapor with H_2 in similar circumstances,[30] the only evidence of any spontaneous reaction being that between Ga_2 and H_2 to afford the cyclic molecule Ga(μ-$H)_2$Ga. The Ga_2H_2 system suggests the possibility of at least five possible isomers **IV**–**VIII** for the Ga_2SiH_4 molecule, dis-

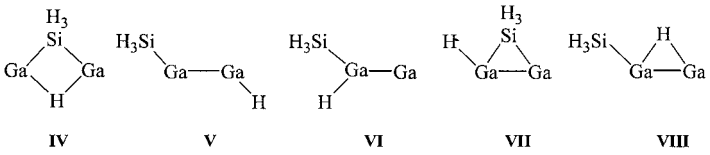

IV **V** **VI** **VII** **VIII**

counting a loosely bonded adduct $Ga_2 \cdots SiH_4$, which would be difficult to reconcile with the IR properties observed for **4b**. Of these, the singlet tricyclic species HGa(μ-SiH_3)Ga (**VII**) is found by DFT calculations to lie lowest in energy, being more stable than *trans*-$HGaGaSiH_3$ (**V**) by 17 kJ mol^{-1}; no stable geometry (without imaginary vibrational frequencies) can be established for models **IV**, **VI**, and **VIII**. The preferred geometry is characterized by a planar HGa(μ-Si)Ga skeleton and conforms overall to C_s symmetry; the dimensions computed for this and the slightly less favored isomer **V** are given in Figure 7. The system

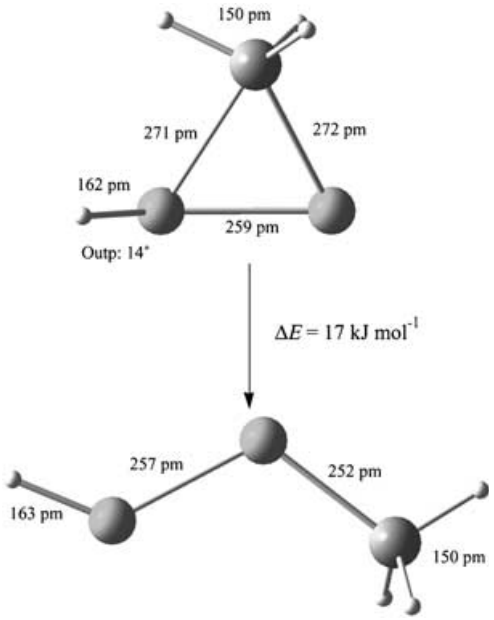

Figure 7. Calculated structures of the two most stable isomers of Ga_2SiH_4.

Ga_2SiH_4 thus contrasts with Ga_2H_2, for which all the corresponding isomers are represented by stable minima on the potential-energy hypersurface; here the global minimum corresponds to the tetracyclic Ga(μ-$H)_2$Ga which, together with $GaGaH_2$ and *trans*-HGaGaH, has been identified experimentally.[30] The instability of **IV** must reflect the incompatibility of the bridging requirements of the H and SiH_3 ligands.

In Table 8 the wavenumbers and IR intensities estimated for the optimum geometries of models **V** and **VII** are compared with the IR properties observed for **4b**. Both models reproduce quite well the essential features of the measured spectra in predicting that the two most intense absorptions should occur near 1700 and 800 cm^{-1}, and it is impossible to distinguish between them on this evidence alone. Our preference for model **VII** is therefore guided by the DFT calculations, although we cannot rule out the possibility that the calculations are insufficiently refined to evaluate reliably the relative energies of the two isomers. It is also possible that the solvating effect of the matrix changes the energy balance, or that kinetic factors associated with the matrix conditions override thermodynamic preferences. Calculations showed that triplet electronic states of the isomers **V** and **VII** lie at higher energies than the corresponding singlet states.

Table 8. Observed and calculated IR wavenumbers [cm^{-1}] and calculated intensities [km mol^{-1}, given in parentheses] of the different isomers of $HGaGaSiH_3$.

Calcd[a]		Obsd
$HGa(\mu\text{-}SiH_3)Ga$	$HGaGaSiH_3$	
2128.5 (86)	2133.7 (100)	2148.6
2072.4 (74)	2126.4 (88)	2138.0
2048.2 (199)	2108.7 (99)	2128.9
1703.1 (473)	1676.9 (518)	1772.0/1751.2
908.5 (43)	913.9 (30)	–[b]
876.0 (8)	897.8 (35)	–[b]
803.3 (269)	807.6 (361)	864.9
445.9 (6)	441.8 (4)	–[b]
317.4 (31)	334.3 (26)	–[b]
280.1 (6)	318.8 (4)	–[b]
255.0 (6)	279.0 (19)	–[b]
215.7 (22)	179.5 (19)	–[b]
163.3 (6)	161.2 (1)	–[b]
127.6 (5)	113.3 (2)	–[b]
121.1 (9)	47.2 (2)	–[b]

[a] DFT calculation using the BP86 method and a TZVPP-type basis set. [b] Too weak to be observed, or obscured.

Although parallels with Ga_2H_2[30] suggest the possibility of isomerization of Ga_2SiH_4 on photoactivation, we have been unable to detect any clear sign of such a change in our experiments. It is possible, therefore, that photodecomposition occurs on irradiation at $\lambda \approx 254$ nm, with regeneration of SiH_4.

these are bonded only weakly, albeit less weakly than the corresponding complex of Al with the less polarizable CH_4 molecule. Photolysis of the complex with light at $\lambda \approx 410$ or ≈ 254 nm then brings about tautomerization to give the M^{II} derivative $HMSiH_3$. The effect of this photolysis is to excite an electron from a valence M *n*p into either an M $(n+1)$s or an M *n*d orbital, both the valence and higher energy orbitals being more or less strongly perturbed by the coordinated SiH_4 molecule. There is some weight of evidence now that the excited $M(^2S)$ or $M(^2D)$ atoms thus formed can insert spontaneously into X–H bonds (where X = H, CH_3, NH_2, or OH) in a solid matrix environment, whereas the same atoms in their ^2P ground electronic state are inert.[15–17,24,25,41–44] The insertion process for SiH_4 [Eq. (5)] is calculated [MP2/BP86]

$$M(^2P)\cdots SiH_4 \longrightarrow \begin{matrix} & \dot{M} & \\ H & & SiH_3 \end{matrix} \qquad (5)$$

to be *exoergic* by 53.6/56.7 and 25.2/17.9 kJ mol^{-1} for M = Al and Ga, respectively. Photolysis of $HMSiH_3$ with light at $\lambda \approx 580$ nm reverses the change, leading back to the adduct $M{\cdot}SiH_4$ [Eq. (1)]. In this respect, the behavior parallels that of the M/PH_3 system in similar circumstances: earlier studies[26] revealed that the adduct $M{\cdot}PH_3$ is converted to $HMPH_2$ by irradiation at $\lambda \approx 440$ nm and regenerated by irradiation of this product at $\lambda \approx 550$ nm.

The conditions of formation and tautomerization of $M{\cdot}SiH_4$ and $HMSiH_3$ allow us roughly to define limits to the barrier to tautomerization. The existence of a significant barrier is made plain by the detection of only the adduct $M{\cdot}SiH_4$ before photolysis. Figure 8 displays the relative energies calculated for the species $M{\cdot}SiH_4$ and $HMSiH_3$ in their ground electronic states and the excited states accessible under the conditions of photolysis applied in this study. The energies of the first excited states of $M{\cdot}SiH_4$ and $HMSiH_3$ are estimated to lie about 290 and 205 kJ mol^{-1}, respectively,

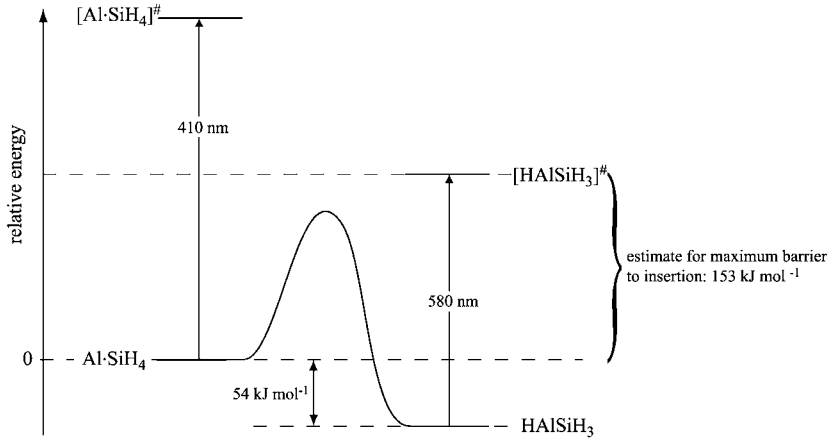

Figure 8. Estimate of the barrier to conversion of $Al{\cdot}SiH_4$ to $HAlSiH_3$ on the basis of selective photolysis experiments and of quantum chemical calculations.

Reaction pathways: According to our experimental results, co-condensation of Al or Ga atoms (M) with SiH_4-doped Ar results in the spontaneous formation of a complex $M{\cdot}SiH_4$. With interaction energies calculated at the MP2 level to be only 5.4 and 8.8 kJ mol^{-1} for M = Al and Ga, respectively,

higher than that of the ground states on the evidence of the experimental selective photolysis results, regardless of whether M = Al or Ga. Taking into account the energy differences of $\approx 54\,kJ\,mol^{-1}$ between $Al{\cdot}SiH_4$ and $HAlSiH_3$ in their ground states, we deduce that $\approx 150\,kJ\,mol^{-1}$ is the upper limit to the barrier to tautomerization (see Figure 8). Similar arguments lead to a value of $180\,kJ\,mol^{-1}$ for the Ga system.

As observed previously with the reaction sequences for the matrix-isolated systems M/H_2[25] and M/CH_4,[15] the insertion product $HMSiH_3$ is not the limit to photochemical change. Instead, it decomposes when exposed to broadband UV-visible light ($\lambda = 200$–800 nm) with fission of the M–H bond, release of H· atoms, and formation of the M^I derivative $MSiH_3$. Scheme 1 summarizes the reaction channels observed in our experiments.

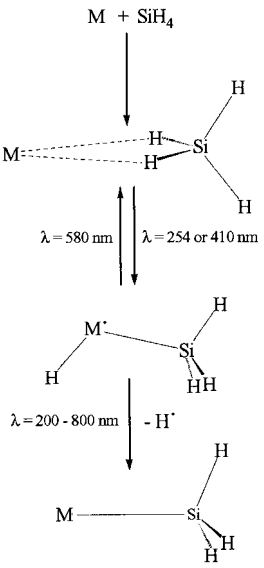

Scheme 1.

The question naturally arises of why we find no sign of the Al counterpart to the digallium compound $HGa(\mu\text{-}SiH_3)Ga$. Possibly Al_2 differs from Ga_2 in its reactivity: more probably the answer concerns matrix concentrations, and the circumstantial evidence that Al_2 is not formed to the same extent as Ga_2. The problem of how Ga_2, which has a triplet $^3\Pi$ ground electronic state, is transformed by its facile reaction with H_2 to a *singlet* product, $Ga(\mu\text{-}H)_2Ga$,[30] has been analyzed elsewhere in some detail.[43] The formally forbidden intersystem crossing necessitated in this case, and presumably also in the reaction with SiH_4, is confronted apparently by a relatively small activation barrier. A more detailed account of the matrix reactivity of M_2 dimers toward SiH_4 and related molecules must, however, await the results of continuing research.[44]

Acknowledgement

The authors thank the Deutsche Forschungsgemeinschaft for financial support of the Karlsruhe group; and the EPSRC for similar support of the Oxford group, including the funding of a studentship for V.A.M., and the award of an Advanced Fellowship to T.M.G. We are indebted to Professor H. Bürger for providing us with a sample of SiH_3D, and also to Professor D. C. McKean for helpful discussions.

[1] a) R. H. Crabtree, *Chem. Rev.* **1985**, *85*, 245; b) U. Schubert, *Adv. Organomet. Chem.* **1990**, *30*, 151; c) R. H. Crabtree, *Angew. Chem.* **1993**, *105*, 828; *Angew. Chem. Int. Ed. Engl.* **1993**, *32*, 789; d) D. G. Musaev, K. Morokuma, *J. Am. Chem. Soc.* **1995**, *117*, 799; e) C. Hall, R. N. Perutz, *Chem. Rev.* **1996**, *96*, 3125; f) A. M. LaPointe, F. C. Rix, M. Brookhart, *J. Am. Chem. Soc.* **1997**, *119*, 906; g) J. Y. Corey, J. Braddock-Wilking, *Chem. Rev.* **1999**, *99*, 175; h) Z. Lin, *Chem. Soc. Rev.* **2002**, *31*, 239.
[2] X.-L. Luo, G. J. Kubas, C. J. Burns, J. C. Bryan, C. J. Unkefer, *J. Am. Chem. Soc.* **1995**, *117*, 1159.
[3] I. Atheaux, B. Donnadieu, V. Rodriguez, S. Sabo-Etienne, B. Chaudret, K. Hussein, J.-C. Barthelat, *J. Am. Chem. Soc.* **2000**, *122*, 5664.
[4] R. Withnall, L. Andrews, *J. Phys. Chem.* **1985**, *89*, 3261.
[5] G. Maier, H. P. Reisenauer, J. Glatthaar, *Chem. Eur. J.* **2002**, *8*, 4383.
[6] N. Legay-Sommaire, F. Legay, *J. Phys. Chem. A* **1998**, *102*, 8759.
[7] P. E. M. Siegbahn, M. Svensson, R. H. Crabtree, *J. Am. Chem. Soc.* **1995**, *117*, 6758.
[8] R. W. Randall, J. B. Ibbotson, B. J. Howard, *J. Chem. Phys.* **1994**, *100*, 7051.
[9] M. D. Brookes, D. J. Hughes, B. J. Howard, *J. Chem. Phys.* **1997**, *107*, 2738.
[10] D. R. Meininger, B. S. Ault, *J. Phys. Chem. A* **2000**, *104*, 3481.
[11] B. S. Ault, *Inorg. Chem.* **1981**, *20*, 2817.
[12] M.-L. H. Jeng, B. S. Ault, *Inorg. Chem.* **1990**, *29*, 837.
[13] S. R. Davis, L. Andrews, *J. Phys. Chem.* **1989**, *93*, 1273.
[14] Z. Mielke, K. G. Tokhadze, *Chem. Phys. Lett.* **2000**, *316*, 108.
[15] H.-J. Himmel, A. J. Downs, T. M. Greene, L. Andrews, *Organometallics* **2000**, *19*, 1060.
[16] a) J. M. Parnis, G. A. Ozin, *J. Phys. Chem.* **1989**, *93*, 1204, 1220; b) R. D. Lafleur, J. M. Parnis, *J. Phys. Chem.* **1992**, *96*, 2429; c) Z. L. Xiao, R. H. Hauge, J. L. Margrave, *Inorg. Chem.* **1993**, *32*, 642; d) L. B. Knight, Jr., J. J. Banisaukas III, R. Babb, E. R. Davidson, *J. Chem. Phys.* **1996**, *105*, 6607.
[17] a) M. A. Lefcourt, G. A. Ozin, *J. Am. Chem. Soc.* **1988**, *110*, 6888; b) M. A. Lefcourt, G. A. Ozin, *J. Phys. Chem.* **1991**, *95*, 2616, 2623.
[18] B. Gaertner, H.-J. Himmel, *Angew. Chem.* **2002**, *114*, 1602; *Angew. Chem. Int. Ed.* **2002**, *41*, 1538.
[19] a) J. L. Duncan, J. L. Harvie, D. C. McKean, S. Cradock, *J. Mol. Struct.* **1986**, *145*, 225; b) D. C. McKean, I. Torto, J. E. Boggs, K. Fan, *J. Mol. Struct.* **1992**, *260*, 27.
[20] See, for example: A. Zumbusch, H. Schnöckel, *J. Chem. Phys.* **1998**, *108*, 8092.
[21] a) R. Ahlrichs, M. Bär, M. Häser, H. Horn, C. Kölmel, *Chem. Phys. Lett.* **1989**, *162*, 165; b) K. Eichkorn, O. Treutler, H. Öhm, M. Häser, R. Ahlrichs, *Chem. Phys. Lett.* **1995**, *240*, 283; c) K. Eichkorn, O. Treutler, H. Öhm, M. Häser, R. Ahlrichs, *Chem. Phys. Lett.* **1995**, *242*, 652; d) K. Eichkorn, F. Weigend, O. Treutler, R. Ahlrichs, *Theor. Chem. Acc.* **1997**, *97*, 119; e) F. Weigend, M. Häser, *Theor. Chem. Acc.* **1997**, *97*, 331; f) F. Weigend, M. Häser, H. Patzelt, R. Ahlrichs, *Chem. Phys. Lett.* **1998**, *294*, 143.
[22] a) R. F. W. Bader, *Atoms in Molecules: A Quantum Theory*, Clarendon Press, Oxford, **1990**; b) F. Biegler-König, *J. Comput. Chem.* **2000**, *21*, 1040; c) F. Biegler-König, J. Schönbohm, D. Bayles, *J. Comput. Chem.* **2001**, *22*, 545; d) F. W. Biegler-König, T. T. Nguyen-Dang, Y. Tal, R. F. W. Bader, A. J. Duke, *J. Phys. B* **1981**, *14*, 2739; e) S. D. Cohen, A. C. Hindmarsh, *Comput. Phys.* **1996**, *10*, 138.
[23] a) D. E. Milligan, M. E. Jacox, *J. Chem. Phys.* **1970**, *52*, 2594; b) R. E. Wilde, T. K. K. Srinivasan, R. W. Harral, S. G. Sankar, *J. Chem. Phys.* **1971**, *55*, 5681.
[24] H.-J. Himmel, A. J. Downs, T. M. Greene, *J. Am. Chem. Soc.* **2000**, *122*, 9793.

[25] a) F. A. Kurth, R. A. Eberlein, H. Schnöckel, A. J. Downs, C. R. Pulham, *J. Chem. Soc. Chem. Commun.* **1993**, 1302; b) P. Pullumbi, C. Mijoule, L. Manceron, Y. Bouteiller, *Chem. Phys.* **1994**, *185*, 13.
[26] H.-J. Himmel, A. J. Downs, T. M. Greene, *Inorg. Chem.* **2001**, *40*, 396.
[27] H. Bürger, A. Rahner, *Vib. Spectra Struct.* **1990**, *18*, 217.
[28] M. A. Douglas, R. H. Hauge, J. L. Margrave, *J. Phys. Chem.* **1983**, *87*, 2945.
[29] R. H. Hauge, J. W. Kauffman, J. L. Margrave, *J. Am. Chem. Soc.* **1980**, *102*, 6005.
[30] a) H.-J. Himmel, L. Manceron, A. J. Downs, P. Pullumbi, *Angew. Chem.* **2002**, *114*, 829; *Angew. Chem. Int. Ed.* **2002**, *41*, 796; b) H.-J. Himmel, L. Manceron, A. J. Downs, P. Pullumbi, *J. Am. Chem. Soc.* **2002**, *124*, 4448.
[31] J. H. Ammeter, D. C. Schlosnagle, *J. Chem. Phys.* **1973**, *59*, 4784.
[32] a) T. J. Marks, W. J. Kennelly, J. R. Kolb, L. A. Shimp, *Inorg. Chem.* **1972**, *11*, 2540; b) T. J. Marks, J. R. Kolb, *Chem. Rev.* **1977**, *77*, 263.
[33] A. J. Downs, T. M. Greene, E. Johnsen, P. T. Brain, C. A. Morrison, S. Parsons, C. R. Pulham, D. W. H. Rankin, K. Aarset, I. M. Mills, E. M. Page, D. A. Rice, *Inorg. Chem.* **2001**, *40*, 3484.
[34] See, for example, the following with the references cited therein: a) D. C. McKean, A. A. Chalmers, *Spectrochim. Acta* **1967**, *23A*, 777; b) A. M. Coats, D. C. McKean, D. Steele, *J. Mol. Struct.* **1994**, *320*, 269.
[35] B. Gaertner, H.-J. Himmel, *Inorg. Chem.* **2002**, *41*, 2496.
[36] P. H. Kasai, H.-J. Himmel, *J. Phys. Chem. A* **2002**, *106*, 6765.
[37] a) D. C. McKean, *Chem. Soc. Rev.* **1978**, *7*, 399; b) D. C. McKean, *J. Mol. Struct.* **1984**, *113*, 251; c) D. C. McKean, *Croat. Chem. Acta* **1988**, *60*, 447.
[38] See, for example: a) M. Brookhart, M. L. H. Green, L.-L. Wong, *Prog. Inorg. Chem.* **1988**, *36*, 1; b) W. Scherer, G. S. McGrady, *Angew. Chem.* **2004**, *116*, 1816; *Angew. Chem. Int. Ed.* **2004**, *43*, 1782.
[39] V. A. Macrae, T. M. Greene, A. J. Downs, *J. Phys. Chem. A* **2004**, *108*, 1393.
[40] L. Andrews, X. Wang, *J. Phys. Chem. A* **2002**, *106*, 7696.
[41] H.-J. Himmel, A. J. Downs, T. M. Greene, *Chem. Rev.* **2002**, *102*, 4191.
[42] A. J. Downs, H.-J. Himmel, L. Manceron, *Polyhedron* **2002**, *21*, 473.
[43] A. Köhn, H.-J. Himmel, B. Gaertner, *Chem. Eur. J.* **2003**, *9*, 3909.
[44] B. Gaertner, H.-J. Himmel, A. J. Downs, V. A. Macrae, unpublished results.

Received: September 1, 2003
Revised: November 14, 2003
Published online: May 18, 2004

